Capacities and Irreversibility of the Vapour Compression Refrigeration System's Components using Aluminium oxide (Al_2O_3) based Nanolubricants

M. Ogbonnaya[1, 2]*, O. O. Ajayi[1], M.A. Waheed[1, 3]

[1] Department of Mechanical Engineering, Covenant University, Ota, Ogun State, Nigeria
[2]Department of Mechanical Engineering, University of Lagos, Akoka, Lagos State, Nigeria.
[3]Department of Mechanical Engineering, Federal University of Agriculture, Abeokuta, Ogun State, Nigeria.

ABSTRACT: Hydrochlorofluorocarbon and chlorofluorocarbon refrigerants commonly used in vapour compression refrigeration system (VCRS) have been phased out due to their negative impact on the ecosystem. R134a and R600a refrigerants were considered as their replacement, but they possess low thermal properties, thereby affecting the performance of the VCRS. In this study, the effect of varying aluminium oxide (Al_2O_3) nanoparticle size (10 nm, 20 – 30 nm and 80nm) and volume concentration (1%, 3%, 5% 10% and 20%) on the capacity and exergy efficiency of each component of VCRS for the optimisation of the VCRS performance and reduction of energy consumption was analysed using R134a and R600a refrigerants. The nanolubricant were prepared using the two-step method. The VCRS showed no significant deterioration in the performance of its components as confirmed for over 24 hours when nanorefrigerant was used. The compressor capacity of nanorefrigerant was lower than that of pure refrigerants while the addition of nanoparticle enhanced the refrigeration effect. The exergy efficiency of the vapour compression system improved with the addition of nanoparticles into the system, the exergy destruction caused by friction in the compressor significantly reduced, thereby reducing the energy consumed by the system.

KEYWORDS: Aluminium Oxide, Efficiency, Capacities, Irreversibility, Nanorefrigerant, VCRS

[Received Nov. 16, 2022; Revised March 1, 2023; Accepted April 14, 2023] Print ISSN: 0189-9546 | Online ISSN: 2437-2110

I. INTRODUCTION

The vapour compression refrigeration systems (VCRS) are used in industries and homes for cooling and preservation. Hydrofluorocarbon (HFC), hydrochlorofluorocarbons (HCFC), chlorofluorocarbon (CFC), fluorocarbon (FC), hydrocarbon (HC) and azeotropes are some the of common refrigerants used in VCRS and air conditioners because of its excellent thermophysical properties but the Kyoto protocol classified them as environmentally unsafe because of their negative effects on the ozone layer and emission of greenhouse gases (UNEP, 1997). Due to this, refrigerant experts seek for alternative refrigerants that are eco-friendly with lower green warming potential (GWP), zero ozone depletion potential (ODP) and excellent thermophysical properties. Environmentally friendly refrigerants such as R134a and R600a has lower GWP and ODP but possess lower thermal conductivity (Ogbonnaya *et. al*., 2022). Therefore, there is a need to improve their heat transfer properties to enhance the rate of heat transfer within the system and the surroundings, thereby, enhancing the energy efficient, heat transfer, refrigeration effect, COP, and reduce energy consumed by the system. Other properties that affect the performance and exergy efficiency of the VCRS are the viscosity, density, surface tension, and specific heat capacity of the refrigerants (Patil *et. al*., 2006).

The dispersion of nanoparticles into eco-friendly refrigerant affects the thermal conductivity, density, viscosity, pH, surface tension and thermal properties of the heat transfer fluid (Faizan and Han, 2016; Kushwaha *et. al*., 2016; Ogbonnaya, *et. al*., 2020; Sanukrishna *et. al*., 2017). Mahbubul, *et. al*. (2013) experimentally studied the impact of nanoparticle concentration on the thermal conductivity of nanorefrigerant. The nanorefrigerant was prepared by dispersing Al2O3 of mean diameter 13 nm into R141b refrigerant and the concentrations considered in the analysis was varied from 0.5% to 2%. At 2% concentration, the result revealed an enhancement of 141% when compared with the base R141b refrigerant. Manasa *et. al*., (2021), studied the effect of nanoparticle concentration and temperature on the thermal conductivity of CuO/R600a nanorefrigerants. The thermal conductivity of nanorefrigerant was observed to increase as the temperature of the nanorefrigerant increased. This enhancement was attributed to the increase in Brownian motion. Considering the viscosity of the mixture of copper oxide (CuO) and cerium oxide (CeO2) nanoparticles dispersed in polyolester oil (POE), the viscosity increased as the concentration of CuO/CeO2 nanoparticle increased (Mohamed *et. al*. 2022). Mahdi *et. al*. (2017) reported that the viscosity of

*Corresponding author: mogbonnaya@unilag.edu.ng

doi: http://dx.doi.org/10.4314/njtd.v18i4.1459

Al2O3/R134a nanorefrigerant of nanoparticle size 20 – 30 nm with a volume concentration of 0.01% and 0.02% increased as the concentration increased. An increase of 1.4% and 5.2% was obtained for 0.01% and 0.02% particle concentration, respectively. The increase in viscosity tends to affect the pumping power of the compressor and pressure drop within the VCRS. The nanoparticle size, shape, structure, and type, addition of surfactant, and temperature have significant impact on the thermophysical properties, heat transfer characteristics of the nanorefrigerants (Ali and Salam, 2020; Ogbonnaya *et. al*., 2020).

The effect of nanorefrigerants on the VCRS performance was studied by dispersing 20 nm multiwalled carbon nanotube (MWCNT) in R134b refrigerant (Yang *et. al*., 2015). The results showed an enhancement in the heat transfer when compared with pure R141b and the Nusselt number increased by 40%. The addition of nanoparticles into the refrigerant enhanced the thermophysical properties of the heat transfer fluid and heat transfer characteristics of the VCRS (Kushwaha *et. al*., 2016). The performance of VCRS using CuO/R134a, Al2O3/R134a, ZnO/R152a and TiO2/R600a nanorefrigerant at 0.1%, 0.3% and 0.5% nanoparticles concentration was conducted by Katoch *et. al*. (2022). The results were analysed using Simulink model and the heat transfer characteristics of nanoparticles was observed to be optimal at a lower concentration of 0.1%. Kundan and Singh (2020) studied the influence of volume flow rate on the COP, cooling capacity and energy consumption of the VCRS using Al2O3/R134a nanorefrigerant with nanoparticle size of 20 nm and mass concentration between 0.5% and 1%. The study observed that an increase in the volume flow rate of nanorefrigerant improved that COP and the cooling capacity of the VCRS. Using 0.5 vol% of CuO and Cu/Ag nanoparticles dispersed in R134a, Yilmaz (2020) observed that the highest COP of 20.88% was obtained for Cu/Ag alloy nanolubricant when compared with pure R134a refrigerant. Studying the lubricant and 5.52% higher than CuO nanolubricant. The enhanced COP of Cu/Ag alloy was attributed to the higher thermal conductivity, best anti-friction and anti-wear characteristics of Cu/Ag alloy when compared with CuO and pure lubricant. Studying the energy consumption of Zirconium Oxide-R134a nanorefrigerant (ZrO2/R134a), Baskaran *et. al*. (2022) reported that the energy consumed by ZrO2/R134a was 6.25% lower than pure 134a refrigerant. Using Copper oxide (CuO) of nanoparticle size 20-30 nm dispersed in R600a/R290 refrigerant, Singh and Ansari (2017) study reported that the energy consumption of the VCRS reduced by 13.5% to 19.7% along with temperature drop between 40 oC and 25 oC when nanorefrigerant is used.

The efficiency of engineering systems can never be 100 percent because exergy is found to be destroyed within the system. Therefore, the exergy analysis is a useful tool used in understanding the overall performance of any system and its various components. The model of the thermal performance of VCRS using three nanoparticles (Cu, Al2O3 and TiO2) dispersed in R718 refrigerants was analysed by Mishra (2015). The exergy efficiency of the system using nanoparticles and eco-friendly refrigerant improved from 8% to 32% when compared with pure refrigerants. Considering the exergy destruction in each of the components of the VCRS, it was observed that the destruction was highest in the expansion valve followed by the condenser, compressor, and evaporator. The sub cooler was the most efficient component. In the study conducted by Ajayi *et. al*. (2019) the compressor process of the VCRS using R134a/Al2O3 nanorefrigerant was observed to be higher than pure R134a at the start of the experiment. The greater the value of the exergy of the compression process the better the performance of the system but at 200 minutes, the exergy of the R134a/Al2O3 nanorefrigerant below that of pure R134a. This reinforces the important of analysing the performance and exergy of VCRS using nanorefrigerant over an extended period. Using nanorefrigerant from metallic oxide (Al2O3, TiO2 and ZnO) nanoparticles, Karthick *et. al*. (2020) reported that the exergy efficiency of the VCRS decreased with an increase in evaporator temperature. The increase in exergy efficiency was 7.51%. This improvement was attributed to the lower evaporator temperature and reduced frictional losses in the compressor. The efficiency defect in the components of the VCRS was lower when compared with plain mineral oil. The exergy analysis of the VCRS using different nanoparticles was investigated by Ajayi *et. al*. (2018). The study involved the use of aluminium composite nanolubricant in a refrigerator compressor system. The aluminium-based nanolubricants used were aluminium oxide (Al2O3), aluminium nickel (AlNi), aluminium cobalt (AlCo) and silver aluminium (AgAl) and the results were compared with the conventional base oil (Capella D). From the result obtained, all the nanolubricant/R134a systems performed better than the conventional base oil system except for AgAl-composite. AlNi-composite nanolubricant/R134a system exhibited the highest exergy efficiency. Abdulftah and Tariq (2019) reported that an increase in the percentage of nanoparticles in the base refrigerant will result in decreased system performance. Complete comprehension of the heat transfers and fluid flow behaviour of nanorefrigerants considering the size and concentration of nanoparticles, and type of refrigerant during a phase change is inevitable for the overall development of more energy-efficient design with better heat transfer performance. From the literature reviewed, authors did not consider the combined effect of nanoparticle size and concentration on the capacities and exergy efficiency of each component in the VCRS and how they affect the overall performance of the system. Therefore, this study evaluates the influence of varying nanoparticle size and concentration on capacities and irreversibility of the components of the VCRS along with the overall exergy efficiency of the system. This study is necessary for the optimisation of the VCRS performance and reduction of energy consumption using R134a and R600a refrigerants and irreversibility analysis describes all losses in the system's components and the overall system. The analysis is aimed at determining the maximum performance of the system, identifying the main site of exergy destruction, and showing the direction for potential improvement in VCRS using Al2O3 nanorefrigerant.

II. MATERIALS AND METHODS/METHODOLOGY/EXPERIMENTAL PROCEDURE

Aluminium oxide nanoparticles of nominal size 10 nm, 20 – 30 nm and 80 nm were used in this study. The two-step method was used in the preparation of 1 %, 3 %, 5 %, 10 %, and 20 % mass concentration of nanolubricant. Some of the samples as nanolubricant produced are shown in Figure 1. The appropriate quantity of dry Al_2O_3 was weighed using the digital electronic balance and then dispersed into the lubricant. The sample was transferred to the ultrasonic bath and mixed for 180 min to destroy nanoparticles agglomerates and mixed mechanically for 120 min using the magnetic stirrer to increase the stability of the nanoparticles in the lubricant. Surfactant was not added during the sample preparation.

The volume concentration of nanoparticles in the lubricant was calculated using Eqn. (3.1) (Das, Putra, Thiesen, & Roetzel, 2003).

$$\emptyset = \frac{m_p/\rho_p}{m_p/\rho_p + m_l/\rho_l} \quad (1)$$

where ϕ is the nanoparticle volume concentration (v/v),m_p and m_l are the masses of the nanoparticle and lubricant respectively while ρ_l and ρ_p are liquid phase density of the lubricant and nanoparticle respectively.

Figure 1: Samples of nanolubricants

Figure 2 shows the experimental test rig used in the evaluation of the capacities and exergy analyses of the various components of the VCRS. The test rig consists of the compressor, condenser, evaporator, expansion valve, pressure gauge and temperature data logger. An air-cooled condenser was used and the heat transfer between the fluid and the surrounding relied only on gravity circulation of the ambient air. The condenser selection depended on the capacity of the refrigeration system, the type of refrigerant, the compressor size, and the type of cooling medium available. The inner and outer diameters of the condenser were given as 6.5 mm and 12 mm respectively with an overall length of 9.41 m for the R134a and R600a setup. The tube of the evaporator is made up of copper with an inner diameter of 10 mm and an outer diameter of 13 mm. The K-type thermocouples were used to measure the temperature at the inlet and outlet of the condenser while for the evaporator, two K-type thermocouples were placed at the inlet and outlet of the evaporator to measure the temperatures of the working fluid. Reciprocating compressor for R134a and R600a were used to compress and pressurize gaseous refrigerant flowing out of the evaporator. The compressors are hermetically sealed type. The suction and discharge pressure of the compressor was measured with two pressure gauges placed at the inlet and outlet of the compressor. A throttling device made up of copper was used to suddenly contract and expand the liquid nanorefrigerants, thereby causing some of the liquid to change into a gas state at constant enthalpy. The throttling device also controls the quantity of the refrigerant that should enter the evaporator subject to the refrigeration load. The refrigerator setup was positioned on a platform in an air-cooled room. The temperature and pressure of the room were at atmospheric conditions. The system was thoroughly checked for leaks before it was charged. The experiment was conducted over a period of 24 hours per sample.

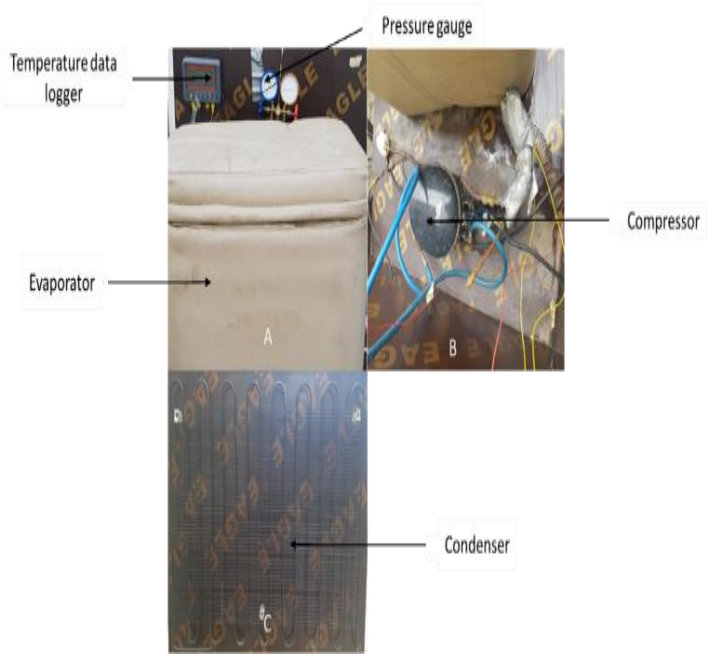

Figure 2: Experimental Test Rig (A) Front View (B) Side view (C)

The capacity analysis of the various components of the vapour compression refrigeration system is essential in evaluating the overall performance of the vapour compression refrigeration system. The capacity of the condenser and evaporator determines the rate at which heat is given out or absorbed by the refrigerant during the process of condensation or evaporation respectively while in the compressor, the capacity denotes the amount of work done by the compressor. The capacities of the compressor, condenser, evaporator, and expansion valve were obtained from Eqns. (2), (3), (5) and (6) respectively (Brasz, 2013; Dinçer, 2003).

The compression capacity is given in Eqn. (2) as:

$$\dot{W}_{comp} = \dot{m}_{nf}(h_2 - h_1) \quad (2)$$

where $\dot{W}_{comp}$ is the compressor power, $\dot{m}_{nf}$ the mass flow rate of the nanorefrigerant and h is the enthalpy.

The condenser capacity $(\dot{Q}_c)$ is given in Eqn. (3)

$$\dot{Q}_C = \dot{m}_{nf}(h_2 - h_3) \quad (3)$$

The refrigeration capacity $(\dot{Q}_E)$ of the system is given in Eqn. (4)

$$Q_E = \dot{m}_{nf}(h_1 - h_4) \quad (4)$$

For the expansion valve

$$h_3 = h_4 \quad (5)$$

The second law of thermodynamics was employed to carry out the exergy analysis of the different components in the system. This analysis describes all losses in the system's components and the overall system. The analysis is aimed at determining the maximum performance of the system, identifying the main site of exergy destruction, and showing the direction for potential improvement. Eqns. (6), (7), (8) and (9) for the compressor, condenser, evaporator, and expansion valve, respectively (Bayrakci & Ozgur; 2009).

Compressor exergy $(\dot{I}_w)$ balance is given in Eqn. (6)

$$\dot{I}_w = \dot{m}_{nf}(h_1 - T_o s_1) - \dot{m}_{nf}(h_2 - T_o s_2) + P_{com} \quad (6)$$

where s is the entropy, T_o is the reference temperature, P_{com} is the compressor power.

Condenser exergy $(\dot{I}_C)$ balance is given in Eqn. (7)

$$\dot{I}_C = \dot{m}_{nf}(h_2 - T_o s_2) - \dot{m}_{nf}(h_3 - T_o s_3) \quad (7)$$

Evaporator exergy $(\dot{I}_E)$ balance is given in Eqn. (8)

$$\dot{I}_E = \dot{m}_{nf}(h_4 - T_o s_4) - \dot{m}_{nf}(h_1 - T_o s_1) + \dot{m}_{nf}(h_1 - h_4)\left(1 - \frac{T_0}{T_E}\right) \quad (8)$$

where T_E is the temperature of the evaporator.

Expansion valve $(\dot{I}_{Exp})$ exergy balance is given in Eqn. (9)

$$\dot{I}_{Exp} = \dot{m}_{nf} T_o (s_4 - s_3) \quad (9)$$

The total exergy (η_{exe}) of the vapour compression refrigeration system is given in Eqn. (10)

$$\eta_{exe} = \left(1 - \frac{I_{total}}{W_{comp}}\right) \times 100 \quad (10)$$

where I_{total} is the total exergy from the different components of the VCRS, W_{comp} is the compressor work.

III. RESULTS AND DISCUSSION

A. Capacities Analyses of the Vapour Compression Refrigeration System's Components Compressor capacity

Figures 3 shows the compressor capacity for R600a for various nanoparticle concentrations and sizes. The compressor capacity of pure R600a was higher than that of Al2O3/R600a nanorefrigerant at all concentrations and sizes except at 20 percent concentration where 20 – 30 nm and 80 nm sized nanoparticles were slightly higher. The work done by the compressor was higher for pure R600a when compared with nanoR600a. This further explains the reason behind the high energy consumption for pure R600a as observed (Ogbonnaya *et. al*. 2023). The average compressor capacity for 10 nm was observed to be lower than other nanoparticle sizes, thereby, making 10 nm more suitable for use in the VCRS also considering the enhanced performance of the system (Ogbonnaya *et. al.*, 2023). Considering the trend of the compressor capacity with respect to the concentration, it can be observed that the minimum compressor capacity of 0.23954 kJ/s, 0.3065 kJ/s and 0.3241 kJ/s was observed for 10 nm, 20 – 30 nm and 80 nm Al2O3/R600a nanorefrigerants at a concentration of 5 percent, 10 percent, and 1 percent respectively. A compressor capacity of 0.3755 kJ/s was obtained for pure R600a refrigerant. At a higher concentration and particle size, the viscosity increases thereby causing the compressor to do more work in pumping the nanolubricant (Ogbonnaya *et. al.*, 2020). Thus, it can be inferred that size and concentration have an impact on compressor capacity.

The compressor capacity for pure R134a and Al2O3/R134a nanorefrigerants is presented in Figure 4. The compressor capacity of Al2O3/R134a nanorefrigerant was found to be lower than that of pure R134a at all concentrations. This implies that more work will be required to compress and pump pure R134a refrigerant into the condenser.

The least compressor capacity considering each nanoparticle size are given as 0.4710 kJ/s for 10 nm at 5%, 0.5434 kJ/s for 20 – 30 nm at 20% and 0.4310 kJ/s for 80 nm at 20%. The value of 0.7524 kJ/s was obtained for pure R134a refrigerant. Across the nanoparticle sizes and considering the average compressor capacity, it can be deduced that 20 – 30 nm sized Al_2O_3/R134a nanorefrigerant required the least work in compressing the nanorefrigerant. This explains why the coefficient of performance of 20 – 30 nm sized Al_2O_3/R134a nanorefrigerant was high and the power consumption was low (Ogbonnaya *et. al*., 2023). Amongst the nanoparticle sizes, the compressor capacity for 10 nm was the highest. This observed trend, strongly suggests that the lubricity of the nanolubricant plays a significant role in compressor capacity. Therefore, a tribological study of nanolubricant needs to be conducted to fully understand the relationship between the nanoparticle concentration and size on the lubricity of the nanolubricant and compressor capacity of the VCRS.

The compressor capacity for pure R600a and its nanorefrigerant was observed to be lower than that of pure R134a and its nanorefrigerants. This further gives reasons as to why R600a and its nanorefrigerant consumed less energy. The compressor capacity of nanorefrigerant was lower than that of pure refrigerants. This implies that less work will be required in compressing and pumping the nanorefrigerant into the condenser. In the compressor, work is not only required in compressing and pumping the refrigerant, but it is also required in overcoming friction within the moving part of the compressor. The viscosity of the nanorefrigerant plays a vital role in determining the compressor capacity of the VCRS. The higher the viscosity, the higher the work required in compressing and pumping the refrigerant into the condenser but from (Ogbonnaya *et. al*., 2020), it can be deduced that the viscosity of pure refrigerant is lower. For pure refrigerants, it is expected that the low viscosity will imply a lower compressor capacity, but this trend was not observed. Sanukrishna *et. al*. (2017), confirmed that the low concentration of nanoparticles dispersed in synthetic oil enhanced the tribological properties of the compressor oil (base oil). This further highlights the fact that the lubricity of a lubricant is as important as its viscosity. From the result obtained, it is suggested that the work required to overcome friction in the moving part of the compressor is higher due to the low lubricity of pure refrigerant.

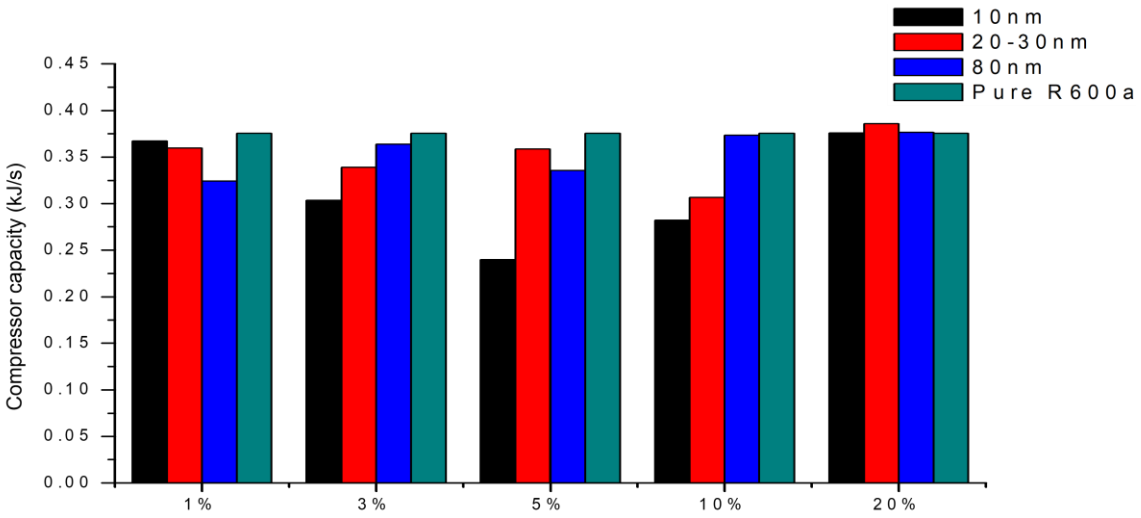

Figure 3: Average compressor capacity at varying volume concentrations of Al_2O_3/R600a nanorefrigerant and pure R600a. Back view

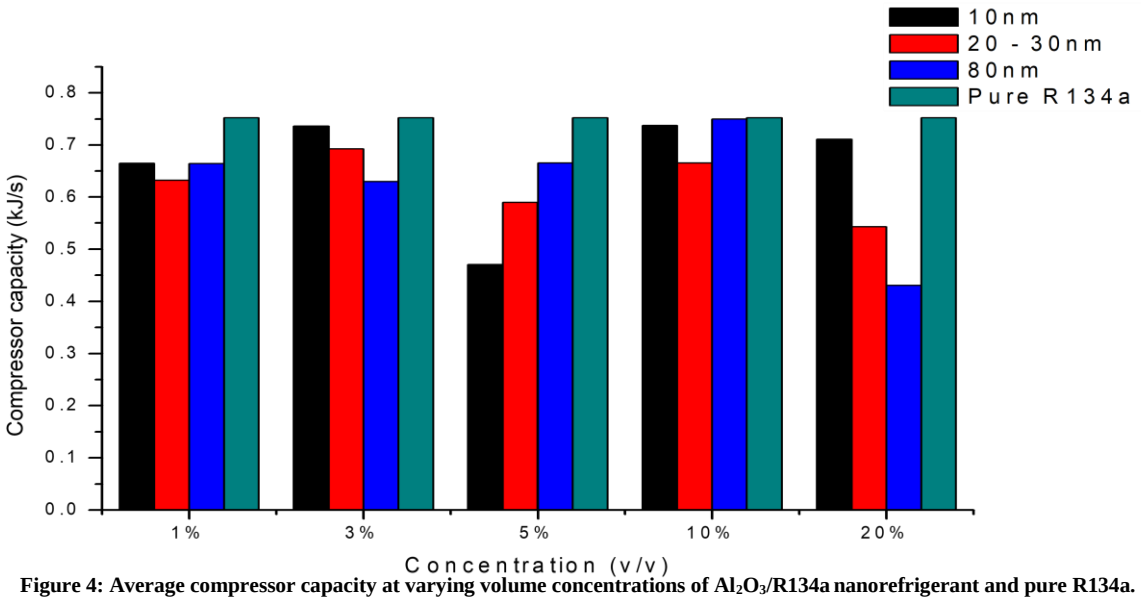

Figure 4: Average compressor capacity at varying volume concentrations of Al_2O_3/R134a nanorefrigerant and pure R134a.

1) Condenser capacity

The condenser of a vapour compression refrigeration system removes heat from the refrigerant to reduce the temperature of the liquid refrigerant below the saturation temperature. The condenser capacity determines the rate at which heat is removed from the refrigerant to condense it from vapour to liquid. Reducing the temperature of the refrigerant increases the refrigeration effect thereby improving the performance of the VCRS.

Figure 5 shows the condenser capacity of pure R600a and Al_2O_3/R600a nanorefrigerant for different concentrations and sizes. On average, the condenser capacity of pure R600a and 80 nm-Al_2O_3/R600a nanorefrigerants were observed to be high. The high condenser capacity indicates that the temperature difference between the refrigerant and the condensing medium is high. Therefore, the higher the temperature difference, the higher the rate at which heat is removed from the refrigerant to the surrounding. From the result obtained, the addition of nanoparticles into the refrigerant reduced the condenser capacity except in few concentrations. The amount of heat removed from pure R600a is obtained as 1.2737 kJ/s. The lowest condenser capacity for 10 nm, 20 – 30 nm and 80 nm had a value of 0.9117 kJ/s, 0.8412 kJ/s and 1.1049 kJ/s at a concentration of 3%, 20% and 1%, respectively.

Figure 6 shows the condenser capacity for pure R134a and Al_2O_3/R134a nanorefrigerants. The condenser capacity of Al_2O_3/R134a nanorefrigerant at all nanoparticle size was observed to be higher than that of pure R134a at 10 percent concentration. Considering the nanoparticle sizes, it was observed that the condenser capacity increased as the nanoparticle concentrations increased but there was a sharp decrease at 5 percent concentration, after which the condenser capacity increased at 10 percent concentration and decreased again at 20 percent concentration. The condenser capacity of pure R134a was obtained as 2.3601 kJ/s while the percentage

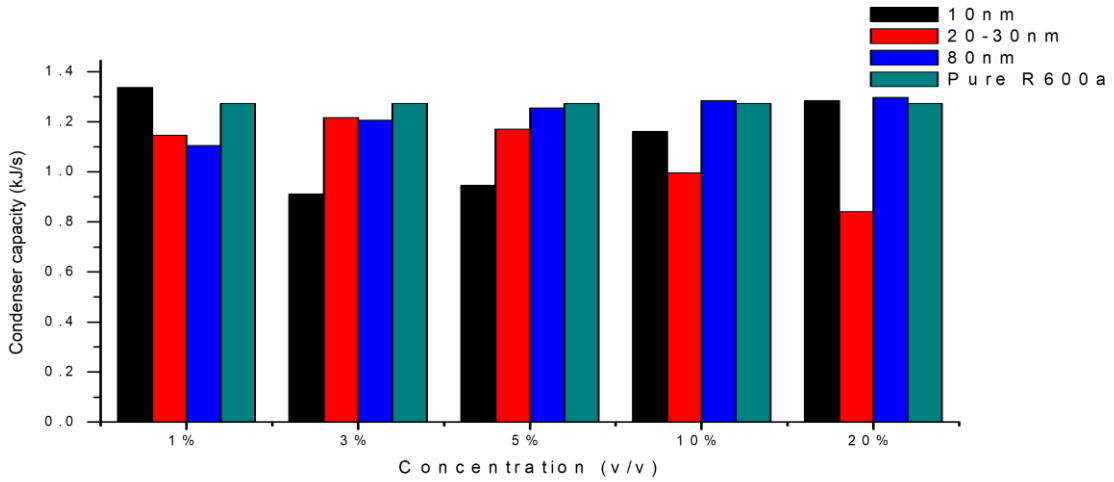

Figure 5: Average condenser capacity at varying volume concentrations of Al_2O_3/R600a nanorefrigerant and pure R600a.

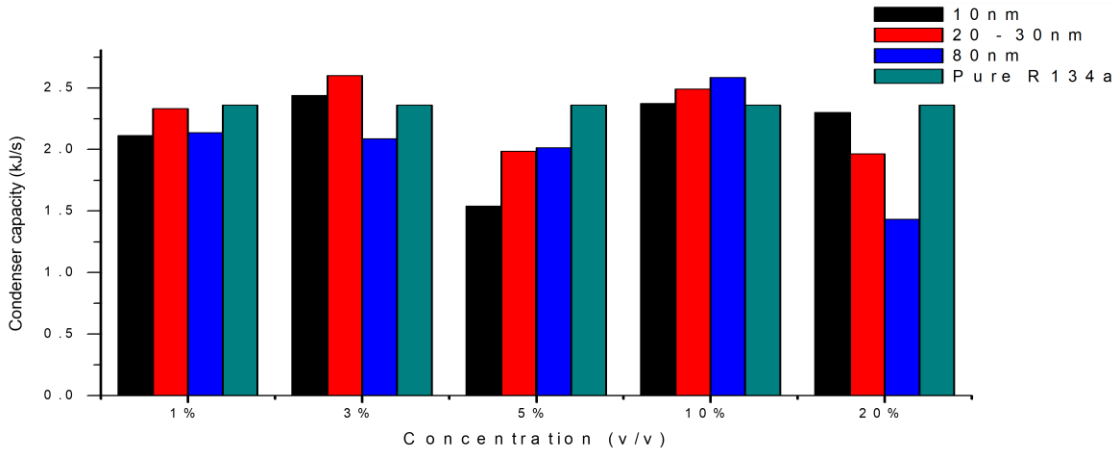

Figure 6: Average condenser capacity at varying volume concentrations of Al_2O_3/R134a nanorefrigerant and pure R134a.

fluctuation of the condenser capacity when compared with that of pure R134a.

The addition of nanoparticles reduced the condensing temperature across the condenser. This trend was also obtained in the research conducted by Kunda and Singh (2020) using Al_2O_3/R134a nanorefrigerant with a nanoparticle size of 20 nm and mass concentration of 0.5% and 1%. The substantial drop in the condenser temperature reduces the condenser capacity. The rate at which heat is removed from the condenser of the vapour compression refrigeration system affects the temperature that the refrigerant will enter the evaporator. Therefore, the condenser capacity determines the refrigeration effect and the overall performance of the system. The condenser capacity of pure R134a and its nanorefrigerant was observed to be lower than that of pure R600a and its nanorefrigerants.

2) Refrigeration capacity

The refrigeration capacity is the rate of heat absorbed from the evaporator space to change the phase of the refrigerant from liquid to vapour. In Figure 7 the refrigeration effect of pure R600a was observed as 0.8982 kJ/s. The refrigeration capacity of 80 nm sized nanorefrigerant was observed to be higher than that of pure R600a at higher concentrations. The refrigeration capacity of the evaporator determines the performance of the VCRS. A high refrigeration effect is desired in the system. The refrigeration capacity of 10 nm and 80 nm were found to increase as the nanoparticle concentration increased except at 1 percent concentration where the refrigeration capacity of 10 nm was found to be higher.

Figure 8 shows that the refrigeration capacity of 20 – 30 nm dispersed in R134a was higher than that of 10 nm and 80 nm sized nanoparticles but at a higher concentration of 10 percent and 20 percent, it was observed that 80 nm and 10 nm were higher, respectively. The crystalline nature of 20 – 30 nm is suggested to be the reason behind its varying behaviour in hydrocarbon and HFC refrigerants. The refrigeration effect was observed to increase as the nanoparticle concentration increased but there was a sharp decrease at 5 percent concentration after which it increased as the concentration increased. This same trend was observed in condenser capacity analysis. Sharma and Rana (2015) stated that the refrigeration effect increased with the increase in concentration but in this study, the relationship between the refrigeration effect and concentration is nonlinear.

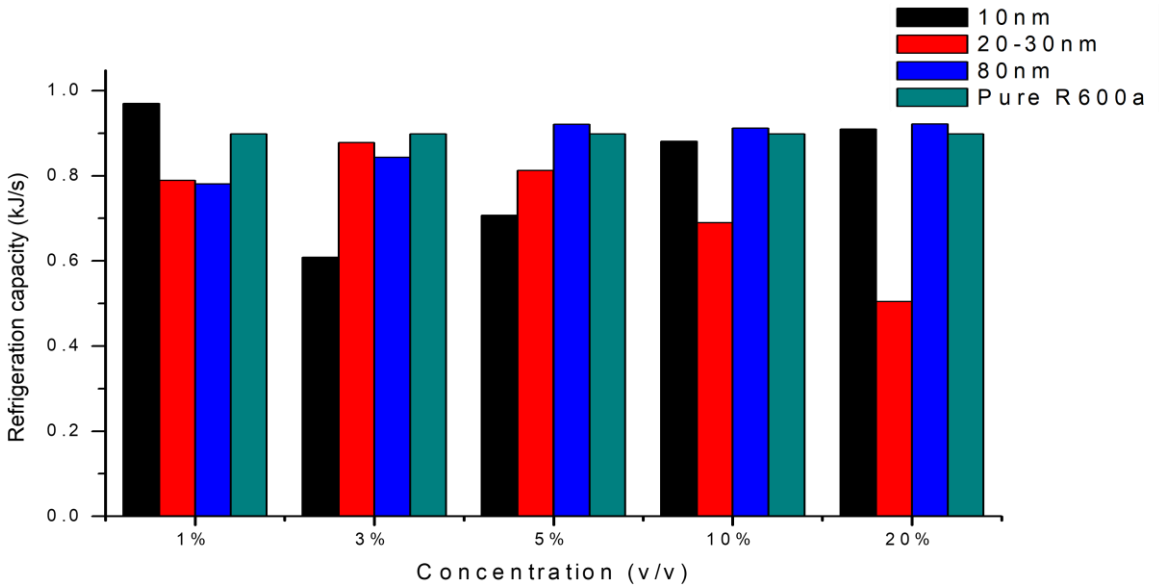

Figure 7: Average refrigeration capacity at varying volume concentrations of Al_2O_3/R600a nanorefrigerant and pure R600a.

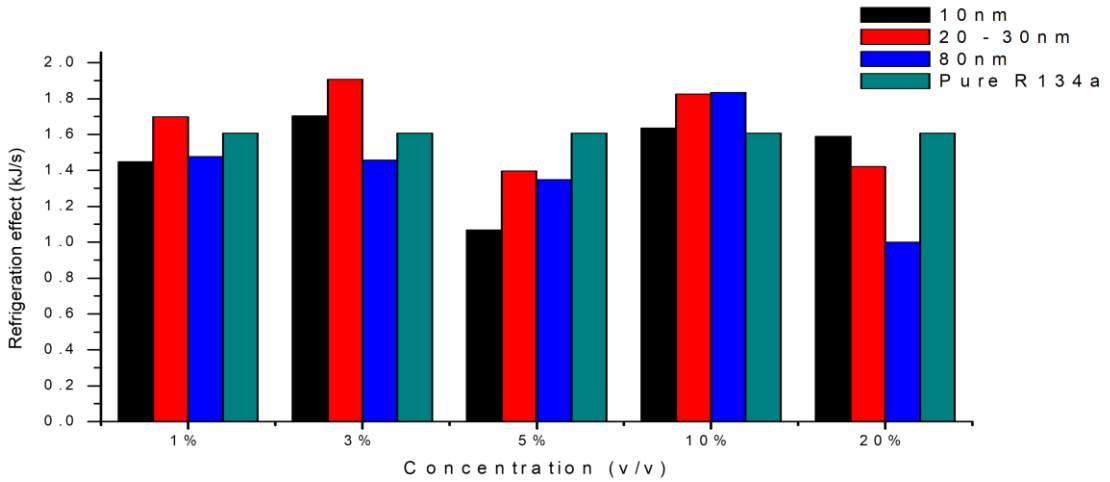

Figure 8: Average refrigeration capacity at a varying volume concentration of Al_2O_3/R134a nanorefrigerant and Pure R134a

B. Exergy Analysis of Vapour Compression Refrigeration System

1) Compressor exergy

The compressor is a major component in the vapour compression refrigeration system which aids in circulating the refrigerant through the VCRS and increases the vapour pressure of the refrigerant to create a pressure difference between the condenser and the evaporator. Figure 9 shows the average compressor exergy for R600a, for many sizes and concentrations of Al_2O_3/R600a nanorefrigerants. In most cases, it was observed that pure R600a refrigerant had the highest compressor exergy destruction when compared with nanorefrigerant except at 20% where 20 – 30 nm sized nanorefrigerant had the highest.

Comparing the compressor exergy destruction across the various nanoparticle sizes with that of pure R600a, it is observed that 20 – 30 nm had the highest compressor exergy destruction of magnitude above pure R600a at 20 percent concentration while 10 nm had the least compressor exergy destruction below pure R600a at 5 percent concentration. On average, it is concluded that the compressor exergy destruction increased as the nanoparticle size increased. Therefore, 10 nm nanoparticles sized Al_2O_3 was observed to possess the least average exergy destruction while pure R600a had the highest exergy destruction.

Considering the nanoparticle concentration, the exergy destruction in the compressor decreases as the concentration decreases for 10 nm and 80 nm but above 5 percent concentration, the compressor exergy destruction increases. Therefore, it can be concluded that 10 nm and 80 nm sized nanoparticles had the least exergy destruction at 5 percent concentration, while 20 – 30 nm had the least exergy destruction at 10%. The highest exergy destruction in the compression occurred at 1 percent and 20 percent concentration. This can be attributed to the viscosity and lubricity of the fluid.

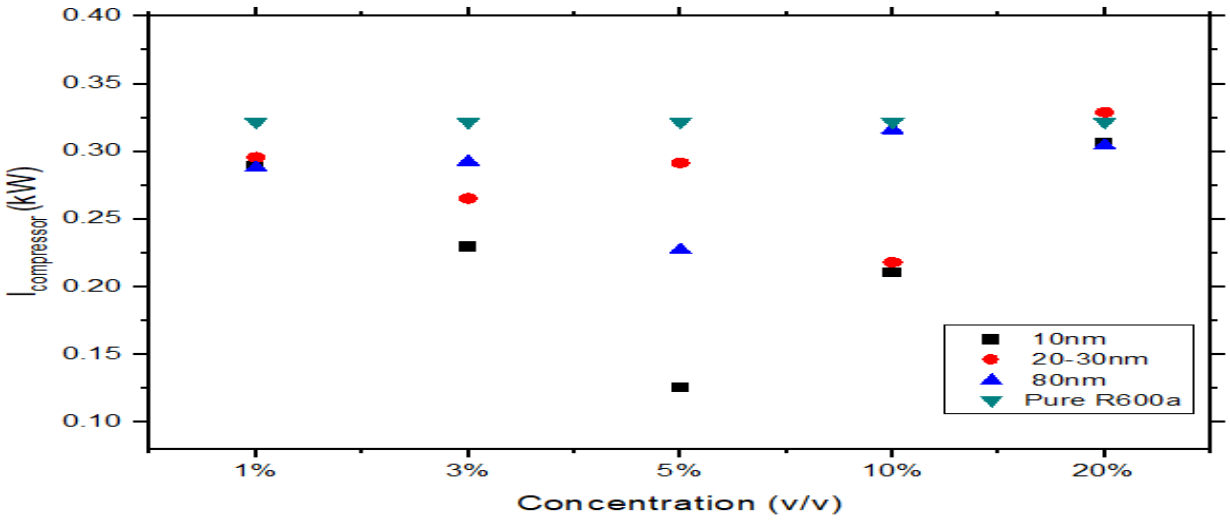

Figure 9: Average compressor exergy destruction for varying volume concentrations of Al_2O_3/R600a nanorefrigerant and pure R600a.

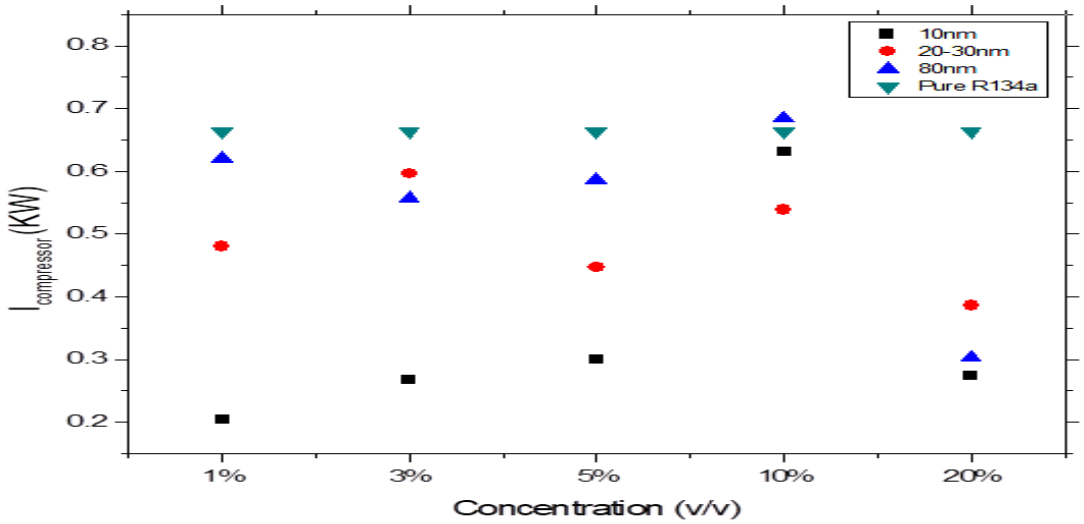

Figure 10: Average compressor exergy destruction for varying volume concentrations of Al_2O_3/R134a nanorefrigerant and pure R134a.

The average compressor exergy for R134a for various concentrations and nanoparticle sizes is shown in Figure 10. Pure R134a had the highest compressor exergy destruction at all concentrations except at 10 percent concentration where 80 nm had the compressor highest exergy destruction. Comparing the compressor exergy destruction across the various nanoparticle sizes with that of pure R134a, it is observed that 80 nm had the highest exergy destruction above pure R134a at 10 percent concentration while 10 nm had the least compressor exergy destruction below pure R134a at 1 percent concentration. Therefore, less exergy is destroyed in the compressor when 10 nm sized nanoparticle was used in the vapour compression refrigeration system. On average, 10 percent concentration had the highest exergy destruction across the different nanoparticle sizes while 20% concentration had the least.

The existence of friction in the moving part of the compressor is a source of irreversibility in the compressor. From the result obtained from the analysis of R600a and R134a, it is found that the addition of nanoparticles into the compressor oil improves the lubricity of the lubricant, thereby reducing the friction in the moving part. This causes a reduction in the exergy destruction and thereby make useful energy available for use in the VCRS; this further improves the performance of the system. The irreversibility was found to be lower at a smaller nanoparticle size of 10 nm and increases as the nanoparticle size increased. The increase in irreversibility can be attributed to the higher viscosity of nanolubricant at higher nanoparticle size. It was also observed that the exergy destruction in the compressor was higher for R134a nanorefrigerant when compared with that of R600a.

2) Condenser exergy

The average condenser exergy destruction for R600a and R134a are shown in Figures 11 and 12, respectively. As heat is rejected from the refrigerant to the environment through the condenser, it was observed in Figure 11 that average condenser exergy destruction was higher for nanorefrigerant when

compared with pure R600a except at 10% where 10 nm had the lowest exergy destruction. Considering the nanoparticle concentration, it was observed that the exergy destruction was highest at 5 percent concentration for 10 nm and 80 nm while 20 nm had the highest at 20 percent concentration.

Exergy destruction for R134a is shown in Figure 12, the condenser exergy destruction of 20 – 30 nm was found to be higher than that of pure R134a concentration at all concentration while 10 nm was higher only at 1 percent and 5 percent concentrations. For 80 nm, it was observed that the condenser exergy for 80 nm was negative for all concentrations except at 5 percent and 20 percent concentrations. This implies that there was an increase in entropy generation. Considering the average exergy destruction, it can be concluded that 80 nm had the least exergy destruction while 20 – 30 nm has the highest exergy destruction in the condenser of the vapour compression refrigeration system.

The exergy destruction was found to be higher for R134a nanorefrigerant when compared with R600a nanorefrigerant. The air-cooled type of condenser was used for this analysis and the temperature difference between the surrounding and the refrigerant is a major determinate in exergy destruction when considering the condenser; therefore, further studies need to be conducted to study the effect of ambient conditions such as temperature and humidity on the rate of exergy destruction in the condenser when using nanorefrigerants.

3) Evaporator exergy

Figure 13 shows the average evaporator exergy destruction of R600a for various sizes and concentrations of Al_2O_3 nanoparticles.

Considering the various nanoparticle sizes, it is observed that for 10 nm sized nanoparticle, the exergy destruction increased as the concentration increased but at higher concentrations of 10 percent and 20 percent, a decreased in exergy destruction was observed and a contrary trend was observed with 20 – 30 nm sized nanoparticles. Exergy destruction was observed to decrease as the concentration increased but at a higher concentration of 10 percent and 20 percent concentration, there was an increase in exergy destruction. The trend for 80 nm sized nanoparticle was observed to be inconsistent in the increase in nanoparticle concentration. The increase in the exergy destruction in the evaporator can be attributed to the decrease in the evaporator's temperature.

This increase occurs because of the increasing temperature difference between the evaporator and its surroundings. For each nanoparticle size, 10 nm sized Al_2O_3 nanoparticles at 10% concentration had the least evaporator exergy destruction while 5% had the highest exergy destruction. For 20 – 30 nm nanoparticle size, 5% concentration had the least exergy destruction while 10% had the highest exergy destruction.

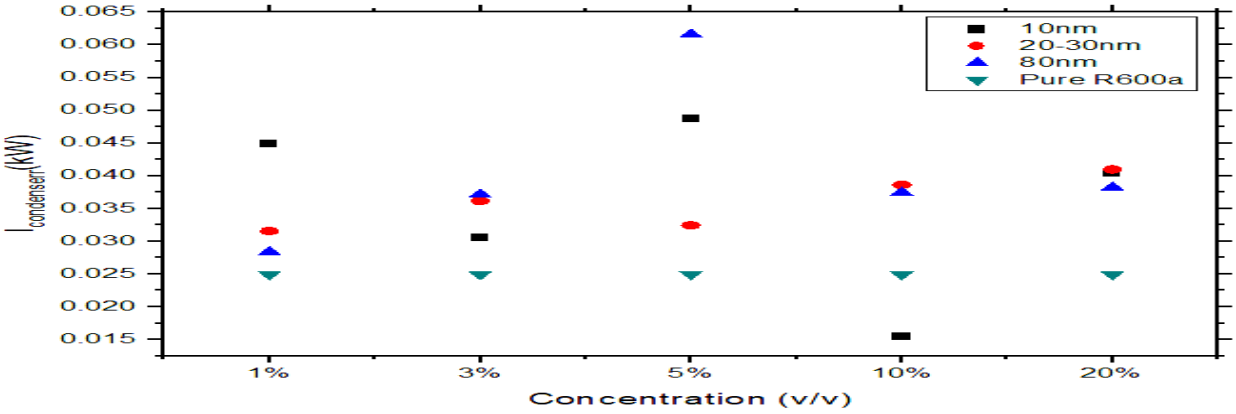

Figure 11: Average condenser exergy destruction for varying volume concentrations of nanorefrigerant and pure R600a.

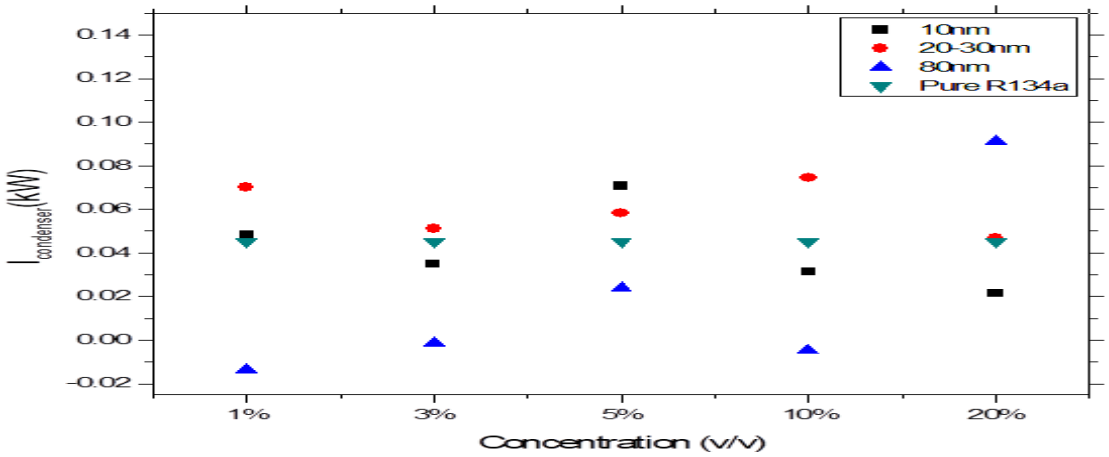

Figure 12: Average condenser exergy destruction for varying volume concentrations of Al_2O_3/R134a nanorefrigerant and pure R134a.

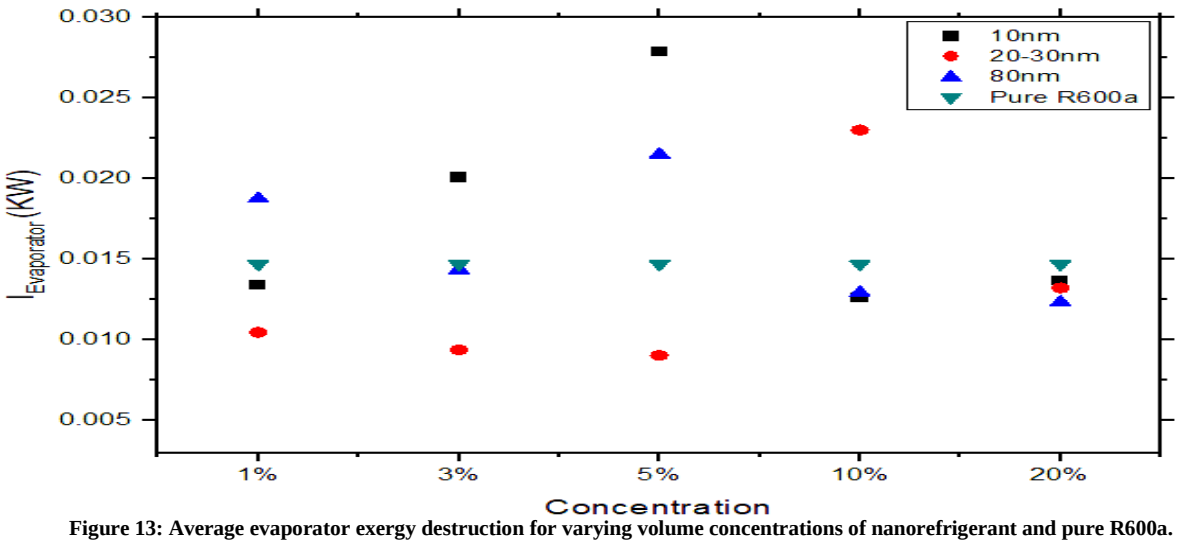

Figure 13: Average evaporator exergy destruction for varying volume concentrations of nanorefrigerant and pure R600a.

For 80 nm, 20% concentration had the least exergy destruction while 5% had the highest exergy destruction, the highest exergy destruction was observed at 5 percent concentration for 10 nm sized while the lowest was obtained at 5 percent for 20 – 30 nm when considering Al_2O_3.

Figure 14 shows the exergy destruction of the evaporator when pure R134a refrigerant and Al_2O_3/R123a nanorefrigerants were used. The result showed that the average exergy destruction in the evaporator for pure R134a refrigerant was higher than that of nanorefrigerant for 10 nm and 20 – 30 nm sized nanoparticles except at 5 percent and 10 percent concentration where 10 nm was higher. On average, the exergy destruction was highest for 80 nm sized nanoparticles. This implies that the exergy destruction in the evaporator increases as the nanoparticle size increased. Considering the destruction with respect to nanoparticle concentration, it was observed that the exergy destruction increased as the concentration increased and at 5 percent concentration, the value obtained for 10 nm was almost the same for pure R134a refrigerant. In summary, 20 - 30 nm sized nanoparticle had the lowest exergy destruction in the evaporator while 80 nm had the highest exergy destruction for varying nanoparticles.

4) Throttle exergy

Considering the throttle exergy destruction for R600a nanorefrigerant as shown in Figure 15, it is observed that the exergy destruction of pure R600a was lower than that of Al_2O_3/R600a nanorefrigerants. On average, the exergy destruction of 20 – 30 nm was higher than that of other nanorefrigerant at higher concentrations. From this analysis, it can be concluded that 5% concentration for nanoparticle size had the highest exergy destruction while 3% had the least exergy destruction.

The 10 nm nanoparticle sized Al_2O_3 had the average least exergy destruction while 20 – 30 nm had the most exergy destruction in the throttle of the vapour compression refrigeration system. Considering 80 nm sized nanorefrigerant, the exergy destruction increased as the concentration increased but decreased after 5 percent concentration, while for 10 nm sized nanorefrigerant the exergy destruction fluctuated as the concentration increased with the highest at 5 percent concentration. For 20 – 30 nm, the exergy increased as the concentration increased.

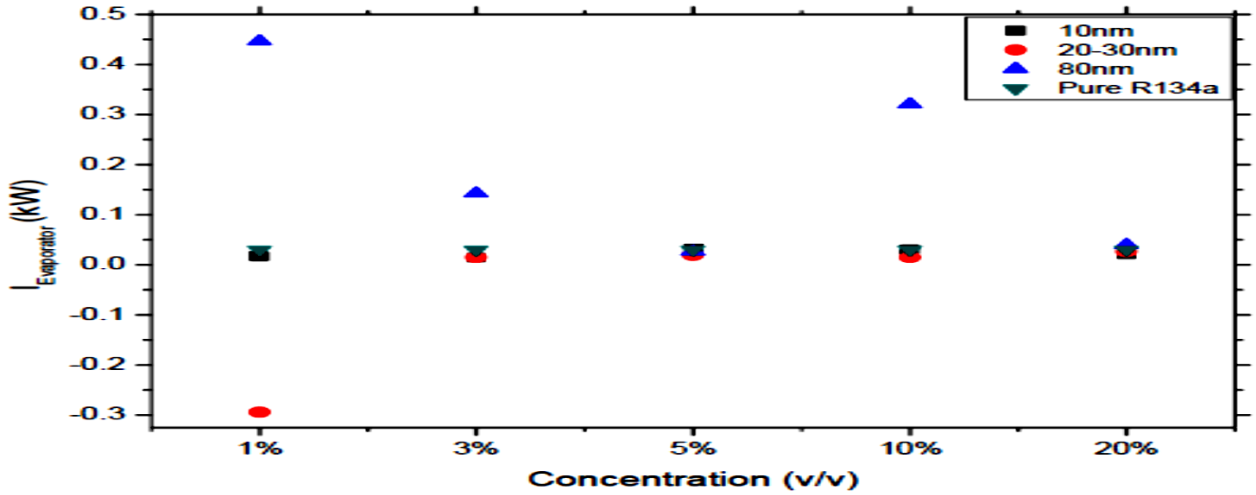

Figure 14: Average evaporator exergy destruction for varying volume concentrations of Al_2O_3/R134a nanorefrigerant and pure R134a.

The average throttle exergy for R134a for various concentrations and nanoparticle sizes is shown in Figure 16. The exergy destruction of pure R134a was found to be lower than that of Al_2O_3/R600a nanorefrigerants for 10 nm and 20 nm sized nanoparticles. The exergy destruction of 80 nm was found to be lower than that of pure R134a refrigerant and the value obtained was found to be negative. The negative sign indicated that the nanorefrigerant was subcooled at the outlet from the throttle and the entropy at that point was higher than that at the inlet. The exergy destruction of 10 nm and 20 – 30 nm nanorefrigerant decreased with the increase in concentration. In summary, considering the average exergy destruction for R134a, 80 nm sized nanoparticles had the lowest exergy destruction in the throttle while 20 – 30 nm had the highest exergy destruction for varying nanoparticles. Comparing the throttle exergy destruction between R600a and R134a nanorefrigerants, it is observed that exergy destruction was higher for R134a when compared with R600a nanorefrigerant.

5) Overall system exergy efficiency

The exergy efficiency of the vapour compression refrigeration system aids in determining and giving insight into the process performance of the VCRS. The exergy efficiency of the whole vapour compression refrigeration system is shown with pure refrigerants and nanorefrigerants is shown Table 1. Considering nanoparticles sizes across various concentration for R600a, 10% concentration for 10 nm had the highest exergy efficiency of 32.10% while 20% concentration for 20 -30 nm had the least exergy efficiency lower than the exergy of pure R600a with efficiency of 24.19%. The exergy efficiency for Al_2O_3/R134a was highest 1% concentration for 10 nm.

IV. CONCLUSION

The combined effect of nanoparticle size and concentration on the optimal performance of the vapour compression refrigeration system considering the capacities and irreversibility analysis of the various components of the VCRS was studied.

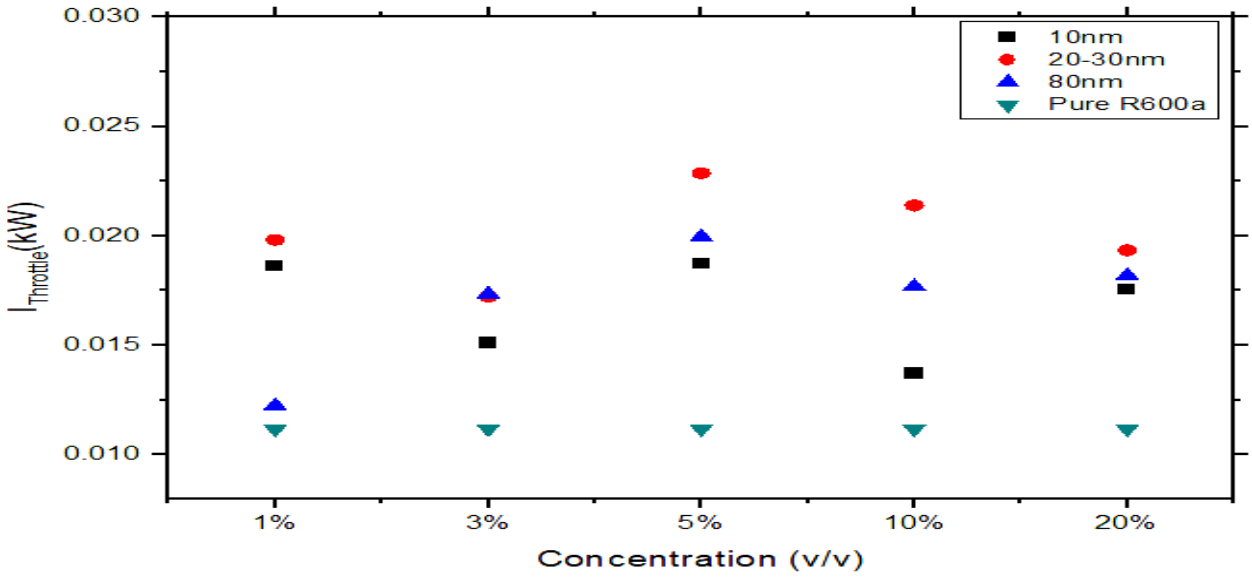

Figure 15: Average throttle exergy destruction for varying volume concentrations of nanorefrigerant and pure R600a.

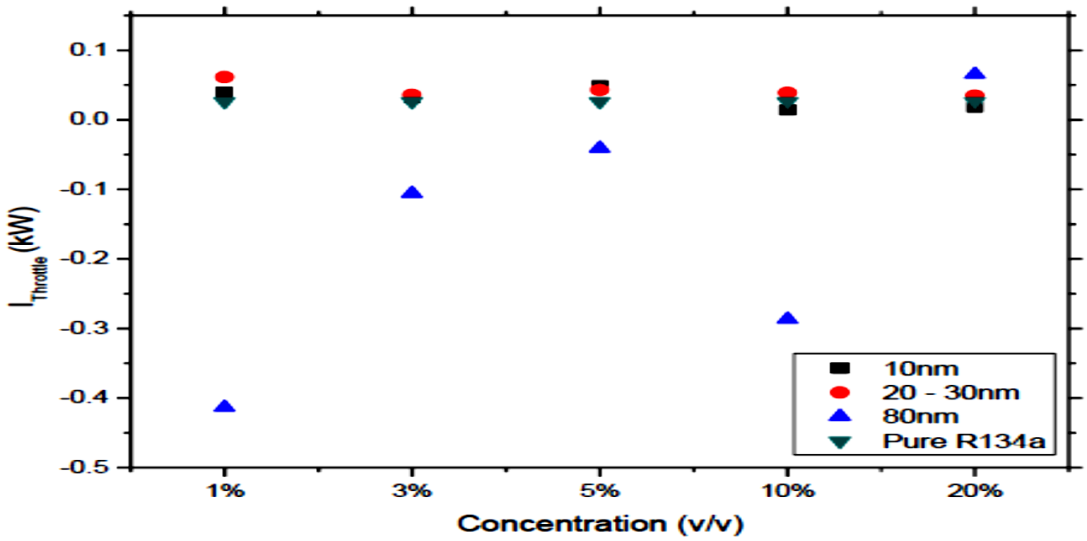

Figure 16: Average throttle exergy destruction for varying volume concentrations of Al_2O_3/R134a nanorefrigerant and pure R134a.

Table 1: Exergy efficiency for varying volume concentrations of nanorefrigerant and pure refrigerants

Concentration	Exergy Efficiency (10 nm)		Exergy Efficiency (20 -30 nm)		Exergy Efficiency (80 nm)	
	R600a	R134a	R600a	R134a	R600a	R134a
0%	24.19	22.12	24.19	22.12	24.19	22.12
1%	23.30	35.61	24.17	31.67	24.26	26.34
3%	25.58	22.96	24.99	22.88	23.82	27.45
5%	30.89	28.90	24.15	26.37	24.46	27.39
10%	32.10	22.12	25.98	26.55	23.26	27.24
20%	23.19	23.66	21.95	30.53	23.31	29.09

The capacities of the components in the VCRS were enhanced with the addition of nanoparticles into the VCRS. The Al2O3 nanoparticles improved the lubricity of the compressor oil, thereby reducing friction, the compressor capacity and the energy required in compressing the refrigerants.

The exergy efficiency of the vapour compression system improved with the addition of nanoparticles into the system. The exergy destruction caused by friction in the compressor was significantly reduced despite the destruction in the compressor was higher when compared with the other components of the VCRS.

The lower nanoparticle size is more efficient when compared with larger nanoparticle sizes. NanoR600a possessed a higher exergy efficiency when compared with nanoR134a.

This study have aided in determining the maximum performance of the system by identifying the main site of exergy destruction, and showing the direction for potential improvement in VCRS when using Al2O3 nanoparticles of different sizes and concentrations.

ACKNOWLEDGEMENT(S)

The authors acknowledge the technical support of Covenant University, Ota in this research.

AUTHOR CONTRIBUTIONS

M. Ogbonnaya: Conceptualization. Methodology, Experiment, Writing. **O. O. Ajayi:** Conceptualization, Supervision, Review and Editing. **M.A Waheed:** Conceptualization, Supervision, Review and Editing.

REFERENCES

Abdulftah, A.K.S. and Tariq M. (2019). Experimental Analysis of Vapor Compression Refrigeration System Using Nano-Refrigerant. World Journal of Engineering Research and Technology, 5 (3): 325-339.

Ajayi, O.O.; T.I. Okolo; Y.S. Enesi; F.T. Owoeye; E.T. Akinlabu; S.T. Akinlabi and S.A. Afolalu. (2019). Performance and Energy Consumption Analyses of R290/Bio-Based Nanolubricant as a Replacement for R22 Refrigerant in Air-Conditioning System. Energy Technology, The Minerals, Metals and Materials Series, Springer, 103 – 112.

Ajayi, O.O.; D.E. Ukasoanya; F.T. Owoeye; E.Y. Salawu; I.O. Ohijeagbon; F. A. Oyawale, and M.C. Agarana. (2018). Experimental Investigation into the Effects of Al-Composite Nanolubricants on the Energy and Exergy Performance of Vapour Compression Refrigerator Compressor. Proceedings of the World Congress on Engineering 2018 Vol II. London, U.K.

Ali, A.R.I. and Salam, B. (2020). A review on nanofluid: preparation, stability, thermophysical properties, heat transfer characteristics and application. *SN Appl. Sci.* **2**, 1636. https://doi.org/10.1007/s42452-020-03427-1.

Baskaran A.; N. Manikandan; JuleLeta Tesfaye, N. Nagaprasad; R. Krishnaraj. (2022). Investigation on the Performance of Domestic Refrigerator with Zirconium Oxide-R134a Nanorefrigerant. Journal of Nanomaterials, vol. 2022, Article ID 3668458, 11 pages, 2022. https://doi.org/10.1155/2022/3668458

Brasz, J.J. (2013). Oil-free centrifugal refrigeration compressors: from HFC134a to HFO1234ze(E), 8th International Conference on Compressors and their Systems, Woodhead Publishing, 467-475.

Das, S. K., Putra, N., Thiesen, P., & Roetzel W., (2003). Temperature dependence of thermal conductivity enhancement for nanofluids. Journal of Heat Transfer, 125(4), 567–574,

Dinçer, I. (2003). *Refrigeration system and application*. John Wiley and Sons, Ltd. ISBN 0-471-62351-2

Faizan, A. and Han, D. (2016). Thermophysical Property and Heat Transfer Analysis of R245fa/Al_2O_3 Nanorefrigerant. The International Journal of Engineering and Science (IJES), 5 (4): 45 – 53.

Katoch A.; F.A. Razak; A. Suresh; B. BS and E. Gundabattini. (2022). Performance Analysis of Nano-Refrigerants used in the Vapor Compression Refrigeration System using MATLAB-Simulink. Proceedings of the Institution of Mechanical Engineers, Part C: Journal of Mechanical Engineering Science, 236 (12):6948-6966. doi:10.1177/09544062211069886

Karthick M.; K. Senthilkumar and K. Varatharajan (2020). Performance Investigation and Exergy Analysis of VCRS Operated Using R600a Refrigerant and Nanoadditive Compressor Oil. Thermal science, 24 (5): 2977 – 2989.

Kumar, R.; D.K. Singh and S. Chander. (2022). A critical review on the effect of nanorefrigerant and nanolubricant on the performance of heat transfer cycles. Heat Mass Transfer 58: 1507–1531. https://doi.org/10.1007/s00231-022-03194-2

Kundan, L. and Singh, K. (2020). Improved Performance of a Nanorefrigerant-Based Vapor Compression Refrigeration System: A New Alternative. Proceedings of the Institution of Mechanical Engineers, Part A: Journal of Power and Energy. https://doi.org/10.1177/0957650920904553

Kushwaha, P.K.; P. Shrivastava and A. K. Shrivastava. (2016). Experimental Study of Nanorefrigerant (R134a+Al_2O_3) Based on Vapor Compression Refrigeration System. International Journal of Mechanical and Production Engineering, 4 (3): 90-95.

Mahdi, Q.S.; M.A. heeb and H. Saed. (2017). Enhancement on the Performance of Refrigeration System using the Nano-Refrigerant. Journal of Energy and Power Engineering, 11: 237-243. DOI: 10.17265/1934-8975/2017.04.004

Mahbubul, I.M., Saidur, R., and Amalina, M.A. (2013). Influence of particle concentration and temperature on thermal conductivity and viscosity of Al2O3/R141b nanorefrigerant. International Communication on Heat Mass Transfer, 43, 100 – 104.

Manasa E.; M.V.S. Murali Krishna and C. I. Priyadarsini. (2021). Enhancement of Thermophysical Properties of Nano Refrigerant, International Journal of Mechanical Engineering and Technology (IJMET), 12 (7): 10-16.

Mishra R. S. (2015) Energy-Exergy Performance Comparison of Vapour Compression Refrigeration Systems using Three Nano Materials Mixed in R718 in the Secondary Fluid and Eco-friendly Refrigerants in the Primary Circuit and Direct Mixing of Nano Materials in the Refrigerants. International Journal of Advance Research and Innovation, 3 (3): 471-477.

Mohamed, H.E.; U. Camdali and M. Aktas. (2022). Viscosity and Density of Polyolester Oils Based on CuO/CeO_2 Mixture Nanoparticles. Acta Scientific Computer Sciences 4.9: 30-39.

Ogbonnaya, M.; O.O. Ajayi and M.A. Waheed (2023). Influence of Refrigerant Type, Nanoparticle's Concentration and Size on the Performance and Exergy Efficiency of the Vapour Compression Refrigeration System Using Al_2O_3 based Nanolubricant. Journal of Nanofluid. Accepted for Publication.

Ogbonnaya, M.; O.O. Ajayi; M.A. Waheed and E.Y. Salawu. (2022). Thermophysical Properties and Heat Transfer Characteristics of Nanorefrigerants: Some Existing Results and Areas for Further Research. Key Engineering Materials. 917: 207-227. doi:10.4028/p-j63e4z.

Ogbonnaya, M.; O.O. Ajayi and M.A. Waheed (2020). Effect of Nanoparticles Size and Concentration on the Thermophysical Properties of Al_2O_3 Nanolubricant for use in Vapour Compression Refrigeration System. Solid State Technology, 63 (6), 7728 – 7739.

Patil, M.S., Kim, S.C., Seo, J., & Lee, M. (2006). Review of the Thermophysical Properties and Performance Characteristics of a Refrigeration System using Refrigerant-Based Nanofluids. Energies, 8: 1 – 16. Doi 10,3390/en9010022

Sanukrishna, S. S.; N. Ajmal and M. Jose-Prakash. (2018). Thermophysical and Heat transfer Characteristics of R134a-TiO_2 Nanorefrigerant: A Numerical Investigation. 28th International Conference on Low Temperature Physics (LT28). IOP Conf. Series: Journal of Physics: Conf. Series 969 (2018) 012015.

Sanukrishna, S.S.; A.S. Vishnu and M. Jose-Prakash, (2017). Nanorefrigerants for Energy Efficient Refrigeration System. Journal of Mechanical Science and Technology, 31: 3993 – 4001.

Sharma, A.K., A.K. Tiwari and A.R. Dixit. (2016). Rheological Behaviour of Nanofluids: A Review. Renewable Sustainable Energy Review, 53: 779–791.

Sharma, T. and Rana, K.L. (2015). An Experimental investigation of nanorefrigerant based refrigeration system. International Journal of Electronics, Electrical and Computational System, 4, 317 – 322.

Singh, B. K. and Ansari, S. (2017). Experimental study of nanorefrigerant (HC+Cu) based refrigeration system. International Journal of Scientific Research in Science, Engineering and Technology, 3 (8): 1076-1076.

UNEP. (1997). Montreal Protocol on Substances that Deplete the Ozone Layer. Final Act. New York: United Nation Environment Program.

Yang, D.; B. Sun; H. Li and X. Fan, (2015). Experimental Study on the Heat Transfer and Flow Characteristics of Nanorefrigerants inside a Corrugated Tube. International Journal of Refrigeration, 56: 213–223.

Yilmaz, A.C. (2020). Performance evaluation of a refrigeration system using nanolubricant. Applied Nanoscience, 10: 1667–1678. https://doi.org/10.1007/s13204-020-01258-5